Images of the Early Universe from the BOOMERanG experiment

P. de Bernardis[1], P.A.R.Ade[2], J.J.Bock[3], J.R.Bond[4], J.Borrill[5,6], A.Boscaleri[7], K.Coble[8], B.P.Crill[9], G.De Gasperis[10], G.De Troia[1], P.C.Farese[8], P.G.Ferreira[11], K.Ganga[9,12], M.Giacometti[1], E.Hivon[9], V.V.Hristov[9], A.Iacoangeli[1], A.H.Jaffe[6], A.E.Lange[9], L.Martinis[13], S.Masi[1], P.Mason[9], P.D.Mauskopf[14,15], A.Melchiorri[1], L.Miglio[16], T.Montroy[8], C.B.Netterfield[16], E.Pascale[7], F.Piacentini[1], G.Polenta[1], D.Pogosyan[4], S.Prunet[4], S.Rao[17], G.Romeo[17], J.E.Ruhl[8], F.Scaramuzzi[13], D.Sforna[1], N.Vittorio[10]

[1] *Dipartimento di Fisica, Universitá di Roma La Sapienza, P.le A. Moro 2, 00185 Roma, Italy,*
[2] *Department of Physics, Queen Mary and Westfield College, Mile End Road, London, E1 4NS, UK,*
[3] *Jet Propulsion Laboratory, Pasadena, CA, USA,*
[4] *CITA University of Toronto, Canada,*
[5] *NERSC-LBNL, Berkeley, CA, USA,*
[6] *Center for Particle Astrophysics, University of California at Berkeley, 301 Le Conte Hall, Berkeley CA 94720, USA,*
[7] *IROE - CNR, Via Panciatichi 64, 50127 Firenze, Italy,*
[8] *Department of Physics, University of California at Santa Barbara, Santa Barbara, CA 93106, USA,*
[9] *California Institute of Technology, Mail Code: 59-33, Pasadena, CA 91125, USA,*
[10] *Dipartimento di Fisica, Universitá di Roma Tor Vergata, Via della Ricerca Scientifica 1, 00133 Roma, Italy,*
[11] *Astrophysics, University of Oxford, Keble Road, OX1 3RH, UK,*
[12] *PCC, College de France, 11 pl. Marcelin Berthelot, 75231 Paris Cedex 05, France,*
[13] *ENEA Centro Ricerche di Frascati, Via E. Fermi 45, 00044 Frascati, Italy,*
[14] *Physics and Astronomy Dept, Cardiff University, UK,*
[15] *Dept of Physics and Astronomy, U.Mass. Amherst, MA, USA,*
[16] *Departments of Physics and Astronomy, University of Toronto, Canada,*
[17] *Istituto Nazionale di Geofisica, Via di Vigna Murata 605, 00143, Roma, Italy,.*

THE CMB AND THE CURVATURE OF THE UNIVERSE

The CMB is the fundamental tool to study the properties of the early universe and of the universe at large scales. In the framework of the Hot Big Bang model, when we look to the CMB we look back in time to the end of the plasma era, at a redshift ~ 1000, when the universe was ~ 50000 times younger, ~ 1000 times hotter and $\sim 10^9$ times denser than today. The image of the CMB can be used to study the physical processes there, to infer what happened before, and also to study the background geometry of our Universe.

The photons of the CMB travel in space for ~ 15 billion years before reaching our

CP586, *Relativistic Astrophysics: 20th Texas Symposium,* edited by J. C. Wheeler and H. Martel

microwave telescopes. Originally visible and near infrared light, they are converted in a faint glow of microwaves by the expansion of the Universe. Since CMB photons travel so long in the Universe, their trajectories are affected significantly by any large-scale curvature of space. The image of the CMB can thus be used to study the large scale geometry of space. The scale of the acoustic horizon at recombination is the "standard ruler" needed for these studies: density fluctuations larger than the horizon are frozen, while fluctuations smaller than the horizon can oscillate, arriving at recombination in a compressed or rarefied state, and thus producing a characteristic pattern of hot and cold spots in the CMB (see e.g. [1] [2] [3] [4] [5]).

In fact, the temperature fluctuations of the CMB are related to the density fluctuations at recombination through three physical processes: the photon density fluctuations δ_γ accompanying the fluctuation of density; the gravitational redshift/blueshift of photons coming from overdense/underdense regions with gravitational potential ϕ; the Doppler shift produced by scatter of photons by electrons moving with velocity v with the perturbation. In formulas (see e.g.[6]):

$$\frac{\Delta T}{T}(\vec{n}) \approx \frac{1}{4}\delta_{\gamma r} + \frac{1}{3}\phi_r - \vec{n}\frac{\vec{v_r}}{c}$$

where n is the line of sight vector and the subscript r labels quantities at recombination. In the CMB temperature distribution we see a snapshot of the status of the density perturbations at recombination: the characteristic size of the horizon in the density fluctuations is thus directly translated in a characteristic size in the spots of the CMB.

Recombination of hydrogen happens when the temperature drops below $\sim 3000K$, i.e. about 300000 years after the Big Bang. The causal horizon is about 300000 light years there. Since the distance travelled by CMB photons is $\sim$ 15 billion light years, and lenghts in the Universe increase by a factor 1000 meanwhile, the angle subtended now by the horizons at recombination is expected to be close to one degree, in a Euclidean Universe. The typical observed angular size of the hot and cold spots strongly depends on the average mass-energy density parameter Ω. The presence of mass and energy acts as a magnifying ($\Omega > 1$) or demagnifying ($\Omega < 1$) lens, producing horizon-sized spots larger or smaller than $\sim 1^o$ in the two cases, respectively.

The image of the CMB is described in statistical terms: the temperature field is expaned in multipoles

$$\frac{\Delta T}{T}(\vec{n}) = \sum_{\ell=1}^{\infty} \sum_{m=-\ell}^{\ell} a_{\ell m} Y_{\ell m}(\vec{n})$$

The $a_{\ell m}$ are random variables with zero average and ensemble variance $< a_{\ell m} a^*_{\ell' m'} >= c_\ell \delta_{\ell\ell'} \delta_{mm'}$. The c_ℓ's represent the angular power spectrum of the CMB. If we compute the power spectrum of the image of the CMB, we expect to see a peak at multipoles $\ell_1 \sim 200$ corresponding to these degree-size spots. The location of the peak will be mainly driven by Ω, thus allowing a measurement of this elusive cosmological parameter. The dependance of ℓ_1 from Ω is not simple in the presently favoured cosmological model with significant vacuum energy Ω_Λ [7] [8]. Full spectral data must be compared to spectral models computed from a set of cosmological parameters, and degeneracies must be taken into account [9], [10]. It remains confirmed, however, that the main driver

for the location of the first acoustic peak is the value of Ω. This can thus be retrieved with good accuracy from the power specturm of an image of the CMB with sub-degree resolution.

After recombination, the same density fluctuations driving the acoustic oscillations grow, and form the jerarchy of structures we see in the Universe today. Thus, the image of CMB anisotropies represents also a fundamental tool in the study of the formation of structures in the Universe.

The detailed shape of the CMB power spectrum c_ℓ has been computed in a number of scenarios with very high detail. A wide literature is available on the subject as well as publically available software ([11], [12]) to accurately compute the power spectrum given a set of cosmological parameters in the framework of adiabatic inflationary models. More work remains to be done for the general case (for example including isocurvature modes, see e.g. [13]).

The main feature, i.e. a harmonic series of peaks following the first one described above, can be understood as follows. The acoustic horizon increases with time, and at some point becomes larger than a given perturbation size. At this point, all the perturbations present in the Universe with that size will start to oscillate. This can be seen as a cosmic synchronization process, which initiates the oscillation of small perturbations before the oscillation of large ones: the phase of the perturbations at the recombination depends on their intrinsic size. Perturbations with size close to the horizon at recombination start last, and have just enough time to arrive to the maximum compression, producing the degree-size spots in the CMB, i.e. the first "acoustic" peak in the angular power spectrum of the CMB anisotropy. Perturbations with smaller intrinsic size have entered the acoustic horizon before, and arrive at recombination after a full compression and a return to the average density. They will produce a CMB temperature fluctuation smaller than the previous ones, because among the three physical processes producing temperature fluctuations from density ones, only the Doppler effect is effective. This corresponds to a dip in the angular power spectrum of the CMB at multipoles larger than the first acoustic peak. Even smaller perturbations have enough time to compress, return to the average density, and then arrive to the maximum rarefaction at recombination, producing a second peak in power spectrum, at multipoles about twice of those of the first one. Repeating this reasoning, we expect a harmonic series of acoustic peaks, up to very small sizes, smaller than the thickness of the last scattering surface. Photons diffusion, and the fact that many small-size positive and negative perturbations are aligned on the same line of sight, damps the temperature fluctuations measurable in the CMB at very high multipoles.

The shape of the power spectrum of the CMB, c_ℓ, depends on several cosmological parameters in addition to Ω. Increasing the physical density of baryons $\Omega_b h^2$ favours compressions against rarefactions in the acoustic oscillations. Compression peaks are thus enhanced with respect to rarefaction ones. The relative amplitude of the second peak (rarefaction) with respect to the amplitude of the first peak (compression) is thus a good measurement of $\Omega_b h^2$. The power spectrum of primordial density fluctuations $P(k)$ controls the general shape of the power spectrum of the CMB. In the inflationary scenario $P(k) = Ak^n$ with $n \sim 1$. The value of n also drives the amplitude of the higher order peaks relative to the amplitude of the first one. If only the first and second peak are observed, increasing n has about the same effect as decreasing $\Omega_b h^2$. A measurement of

the third peak removes this degeneracy.

CMB AND COSMIC INFLATION

In the previous section we have assumed the presence of density perturbations in the primeval plasma. In 1992 the DMR instrument on the COBE satellite has shown that these perturbations do exist at least at large scales[14]. The angular resolution of DMR was 7^o, corresponding to a sensitivity to multipoles between 1 and ~ 20 in the angular power spectrum of the CMB. The power spectrum measured by DMR has a characteristic power spectrum[15] $c_\ell \sim 1/\ell/(\ell+1)$. This is consistent with a Harrison-Zeldovich power spectrum of density fluctuations $P(k) = Ak^n$ with $n = (1.2 \pm 0.3)$.

Such a spectrum is expected in the simplest inflationary scenarios (see e.g. [16] [17] [18] [19] [20]), where microscopic quantum fluctuations in the very early universe ($\sim 10^{-36}$ s after the big bang) are inflated to cosmological scales by the exponential growth of space during an early phase transition at the grand-unification era. The density fluctuations generated in this way are gaussian and adiabatic (see e.g. [21]). Inflation explains the homogeneity of the CMB at large scales: regions causally disconnected at the recombination epoch had been in close causal contact in the very early Universe, before the superluminal inflation of space. Inflation naturally produces a flat geometry of space, stretching any inital curvature, due to the huge expansion factor. The power law spectrum of primordial fluctuations is reminiscent of the initial quantum fluctuations: constraining n through the measurement of the power spectrum is thus a way to test the inflationary hypothesis. However, some inflation variants feature values of $n \sim 0.9$ or even less (see e.g. [22]). The adiabatic inflationary scenario is shown in cartoon form in fig.1.

The alternative scenario for the generation of density fluctuations is based on topological defects (see e.g. [23]). In this scenario non gaussian isocurvature fluctuations are favored. The peak at ℓ_1 is either not present of shifted to higher ℓs. The analysis of the power spectrum and of the image of the CMB (and in particular of its gaussianity properties) can thus distinguish between the two alternative scenarios for the generation of density fluctuations.

The problem of recovering the set of cosmological parameters from the measured power spectrum c_ℓ has been widely studied in view of the satellite missions MAP and Planck, which promise to measure the power spectrum with $\sim 1\%$ accuracy on a very wide range of multipoles, allowing an accurate determination of the main cosmological parameters (see e.g. [25]).

MEASURING THE IMAGE OF THE CMB

The contrast of the image of the CMB is very low ($\sim$ 10 ppm). Moreover, atmospheric and Galactic signals can be much larger than the CMB anisotropy, depending on wavelength, observed sky region and location of the observer. Trying to map the CMB anisotroy from the total brightness coming from the sky in a ground-based exper-

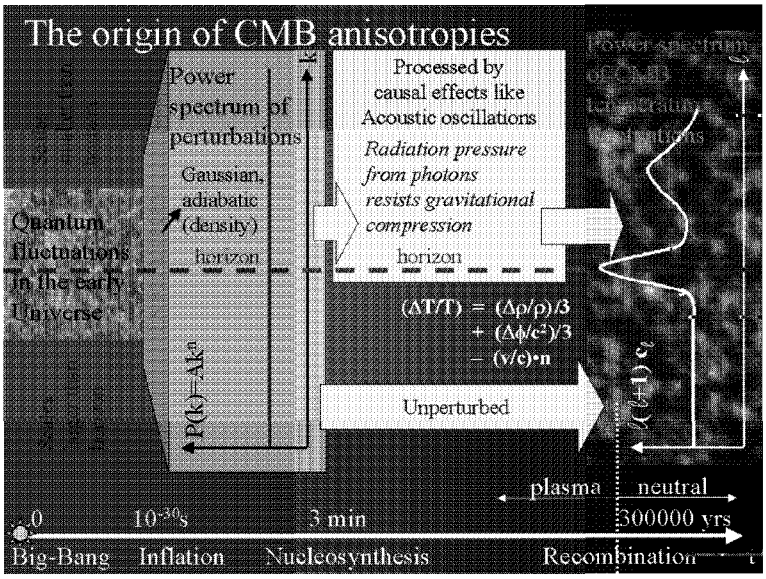

FIGURE 1. Adiabatic inflationary scenario for the generation of CMB anisotropy from quantum fluctuations in the very early universe. Inflation boosts the microscopic fluctuations producing adiabatic gaussian density fluctuations at all cosmological scales. Fluctuatios larger than the causal horizon are effectively frozen, and produce the large scale anisotropy in the CMB measured by the COBE-DMR. Fluctuations entering the horizon before recombination are processed by the cosmological plasma and oscillate as sound waves, thus producing a characteristic power spectrum of anisotropy in the CMB at sub-horizon scales. The angular scale under which these are seen today depends on the curvature of space.

iment is like trying to map distant galaxies in the visual band during daytime. Detector and istrumental noise is an additional problem in these measurements.

For all these reasons, 27 years were needed to produce the first detection of CMB anisotropy after its the discovery. In 1992 the DMR instrument on board of the COBE satellite detected for the first time anisotropy of the CMB at large scales [14]. The resolution of the instrument ($\sim 7^o$ FWHM) was not sufficient to resolve the degree-scale spots useful to measure the curvature of the Universe. Following this detection, many experiments were carried out with degree and sub-degree resolution. The first clear detections of a peak at $\ell \sim 200$ in the angular power spectrum of the CMB anisotropy arrived with the use of new detectors. HEMT based microwave amplifiers [26] [27] were used with the MAT telescope operating at 5000m of altitude in Chile [28] [29]. Spider web bolometers[30] were used at higher frequencies in the test flight of the balloon borne experiment BOOMERanG [31], which was flown in a short flight in Texas in 1997, while TOCO was taking data. Both experiments produced convincing evidence for the peak at $\ell \sim 200$. But the most exciting breakthrough was the recent measurement of wide, resolved images of the CMB, obtained by the BOOMERanG-LDB[32] and by the MAXIMA-1[33] experiments. In the following we will focus on the results from the BOOMERanG experiment.

BOOMERANG

BOOMERanG (Balloon Observations Of Millimeter Extragalactic Radiation and Geophysics) is a 1.3m off-axis scanning telescope using fast, ultra-sensitive bolometric detectors in four frequency bands. The telescope scans the sky at nearly constant speed, of the order of $1^o/s$, along $L_{scan} = 60^o$ wide scans at constant elevation (either 40^o, 45^o, or 50^o). The main beam is similar to a gaussian with $\sigma_{beam} \sim 5'$ at 150 GHz. Different multipoles of the CMB anisotropy are converted by the scan into different audio frequencies in the detectors[34], thus avoiding the effects of 1/f noise and other low-frequency disturbances [35]. This allows the detection of the angular power spectrum over a wide range of multipoles ($\ell_{max} \sim 1/\sigma_{beam}$; $\ell_{min} \sim 1/L_{scan}$) in a single experiment. Two different scan speeds (1 dps and 2 dps) have been used during the measurements to detect possible systematic effects due to the transfer function and noise spectrum of the instrument. The instrument operates in the stratosphere, avoding the large-scale signals and noise produced by atmospheric emission. The full payload is rotated around the vertical axis to avoid scan synchronous instrumental signals. The azimuth of the center of the scan tracks the azimuth of the selected region to be mapped, and sky rotation produces a nicely crosslinked pattern of scans, very useful to reconstrunct the sky map from the time-ordered data. The mesurement is repeated several times in different days, while the instrument drifts by hundreds of kilometers in its stratospheric circumnavigation of Antarctica. This allows the repetition of the measurements under very different experimental conditions, which is the best way to check for systematic effects contaminating the data. For example, every day the ground environment (ice, sea, rocky areas) is different, and so is the ground spillover in the sidelobes of the telescope. A sensitive null test can be obtained by comparing the maps obtained in different days. If the maps are the same, ground spillover contamination can be excluded.

BOOMERanG maps the sky simultaneously at 90, 150, 240 and 410 GHz. Comparison of the maps measured at different frequencies is a powerful tool to test for foregrounds contamination. The two low frequency bands are mainly sensitive to CMB anisotropies, while the two higher frequency bands can be used to monitor atmosperic and interstellar contaminations. 16 detectors have been distributed in the focal plane as shown in fig.2. The location of different detectors in the focal plane has been optimized in order to have robust confirmation of structures in the sky at different time scales.

The technical details of the instrument are reported in [36] and in [37]. The main characteristics are as follows:

- Telescope: off-axis gregorian with cryogenic secondary and tertiary
- Primary mirror: off-axis, aluminum, 45^o off-axis, 1.3m diameter, f/1.
- 90 GHz detectors: 2, 18' FWHM, best $NET_{CMB} \sim 150\mu K\sqrt{s}$
- 150 GHz detectors: 6, 10' FWHM, best $NET_{CMB} \sim 150\mu K\sqrt{s}$
- 240 GHz detectors: 4, 14' FWHM, best $NET_{CMB} \sim 210\mu K\sqrt{s}$
- 410 GHz detectors: 4, 12' FWHM, best $NET_{CMB} \sim 3000\mu K\sqrt{s}$
- Attitude control: azimuth flywheels, passive pendulation damper
- Azimuth scans at 1 to $2^o/s$
- Attitude reconstruction: differential GPS, digital sundial sun sensors, laser gyroscopes

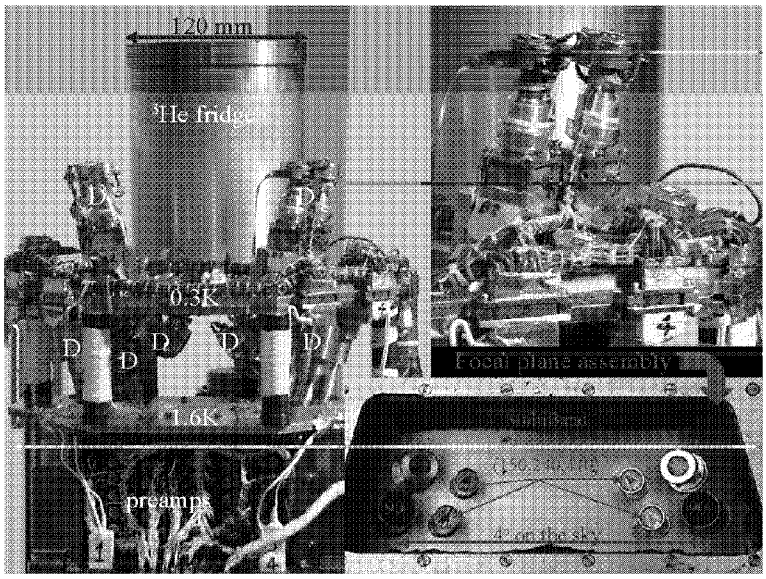

FIGURE 2. The cryogenic focal plane of the BOOMERanG experiment. In the bottom right panel the entrance of the 8 photometers are shown and labeled with the corresponding frequency (in GHz).

The instrument was flown by NASA-NSBF from Dec.29, 1998 to Jan.8, 1999, at 39 Km of altitude, circumnavigating Antarctica at a latitude $\sim -78^o S$. 57 million 16 bit samples were acquired for each detector during the flight.

THE MAPS OF THE MICROWAVE SKY

Maximum likelihood sky maps were constructed from the time-streams using the MADCAP package [38] and a recursive estimator of instrumental noise [39]. The maps cover $\sim$ 1800 square degrees in one of the best (lowest foreground) sky regions in the southern hemisphere. The structures at large angular scales ($\gtrsim 10^o$) have been filtered out to remove the effect of 1/f noise and instrumental drifts. These maps, smoothed to a resolution of 22' FWHM, have been published in [32]. In fig.3 we show sum ($\Delta T_{240} + \Delta T_{150}$) and difference ($\Delta T_{240} - \Delta T_{150}$) maps obtained from the 150 and 240 GHz channels, expressed in CMB temperature fluctuation units. Degree-size structures uniformly covering the surveyed area are the dominant feature of the sum map. The structures disappear in the difference map. This is already a proof of the cosmological nature of the structures.

It is very important to compare the structures visible in the maps at 90, 150 and 240 GHz [32]. The structures are very similar in shape, and the relative amplitude of the fluctuations is perfectly consistent with the derivative of a 2.73K blackbody, as expected for CMB anisotropy. A simple scatter plot of these signals expressed in CMB temperature fluctuations units has best fit slopes very consisten with 1, confirming the visual impres-

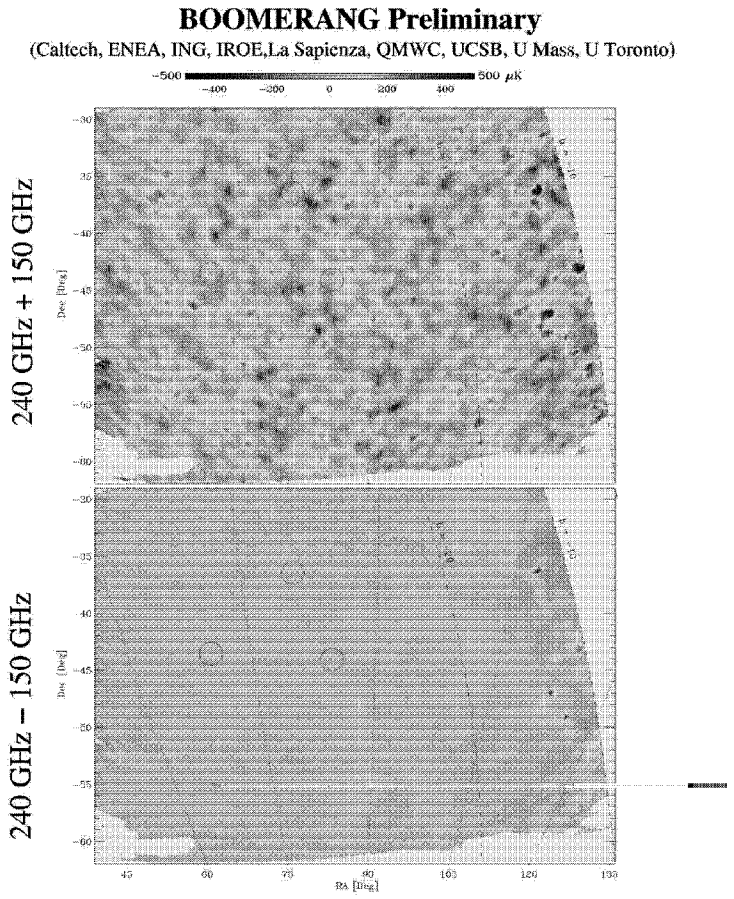

FIGURE 3. The sum (top panel) and difference (bottom panel) maps obtained from the 150 and 240 GHz channels of BOOMERanG. CMB temperature units are used for both the channels. For this reason, CMB fluctuations are enhanced in the sum map, while are removed in the difference map. Only non-CMB structures remain in the difference map. The three circles surround three AGNs present in the map.

sion above[40]. Masi et al. [41] find that the contamination from the main local foreground (i.e. thermal emission from diffuse interstellar dust) is less than 1% of the mean square fluctuation detected at 150 GHz. Moreover, the brightness fluctuations generated by unresolved point-like radio sources can be estimated from existing catalogues ([42]) and is found to be negligible ($\sim 160(\ell/1000)^2 \mu K^2$). From these results we conclude that the dominant feature in the maps is CMB anisotropy, copying the pattern of the acoustic horizons at the last scattering surface. The amplitude of the fluctuations ($\Delta T_{rms} \sim 80 \mu K$) is consistent with the level of CMB anisotropy computed in the inflationary adiabatic

scenario, normalized to the COBE-DMR detection.

The MAXIMA experiment has also produced a map of $\sim 0.25\%$ of the sky at 150 GHz, by observing a high latitude sky region in the Northern Hemisphere [33]. BOOMERanG and MAXIMA nicely complement each other. In fact BOOMERanG covers a large region of the sky, producing data with smaller cosmic variance at $\ell \lesssim 300$, but the precision in the pointing reconstruction is presently limited to 3 arcminutes. For this reason the maps have been smoothed to 22.5' FWHM and the power spectrum is limited to $\ell \lesssim 600$. MAXIMA instead covers a smaller sky region, producing larger errors at multipoles $\lesssim 300$, but has already achieved sub-arcmin precision in the pointing reconstrunction, and the resolution of the map is limited only by the intrinsic resolution on the telescope at $\sim 10'$ FWHM. The power spectrum correspondingly extends up to $\ell \sim 800$. The map from MAXIMA is statistically very similar to the map of BOOMERanG, and this agreement is a very important independent confirmation of the results for both experiments.

THE POWER SPECTRUM OF THE CMB

The angular power spectrum[32] has been computed from the maps of BOOMERanG in two different ways: using a simple spherical harmonics transform [43] and using the MADCAP [38] maximum likelihood algorithm. The two methods produce very consistent results. In fig.4 we report the angular power spectrum of the center region of the BOOMERanG map ($\sim 1\%$ of the sky). together with the data from COBE-DMR and from the recently published MAXIMA, CBI [44] and BIMA [45] experiments.

There are several features immediately evident from these data. The level and shape of fluctuations is consistent with a constant level at the large scales sampled by COBE-DMR, plus a peak due to acoustic horizon effects at scales around one degree. The second peak (and the higher order ones) has not been detected yet, but there is significant power detected at multipoles between 300 and 600. There is a damped tail at multipoles $\gtrsim 1000$, as expected by photon diffusion and line of sight averaging effects at recombination. This behaviour is in remarkable agreement with the simple theory presented in section 2 and we can start to say that the big picture is correct. A word of caution is needed, however. The presence of a second peak is consistent with the current data, but it has not been observed yet. Several experiment promise a detection soon, including the combined analysis of 12 channels in BOOMERanG with refined pointing reconstruction, the second flight of MAXIMA or from the interferometers (DASI [46], CBI [47], VSA [48] etc.) currently getting data. Such detection will be the final proof that the Universe underwent a hot phase with acoustic oscillations, and that the structure we see in the Universe today was grown after the hot plasma phase through gravitational instability from the same primordial fluctuations.

Several experimental problems are immediately evident from the power spectrum shown in fig.4. The data at $50 \lesssim \ell \lesssim 300$ are limited in precision by cosmic variance. This will improve with larger surveys, as in the Archeops [49] and TOPHAT [50] balloon experiments and in the full sky survey of the MAP experiment. Significant calibration errors are still present in the same data sets. A reliable standard of calibration is still

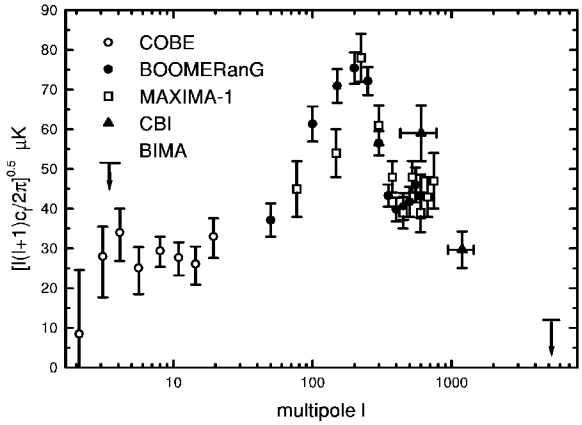

FIGURE 4. Recently published measurements of the angular power spectrum of the cosmic microwave background

non-trivial at these wavelengths, and the Dipole calibration used in BOOMERanG can be affected by scan synchronous effects difficult to monitor to better than 10% [51]. The data at $300 \lesssim \ell \lesssim 600$ are still detector noise limited. In the case of BOOMERanG, this will improve with the simultaneous analysis of all the 12 detectors sensitive to CMB anisotropy (the published power spectrum has been computed from the best detector alone).

The BOOMERanG results have been obtained from a preliminary pointing solution. Jitter in the telescope pointing is a relevant concern, and we are currently working on the development of a refined pointing solution. The main effect of pointing jitter is to spread the equivalent beam of the telescope. In fig.5 we compute the effect of changing the equivalent beam on the most inportant features detected in the spectrum: the location of the peak, its amplitude, and the ratio between the general level of fluctuations at $\ell > 300$ and the amplitude of the peak. It is evident from the figure that the measurement of the location of the peak (controlling the measurement of Ω) is very robust, while the other two quantities (controlling for example the measurement of $\Omega_b h^2$) are less robust.

The present data from the interferometers at $\ell \gtrsim 600$ suffer for lack of spectral resolution and are still single frequency. Moreover, only differential maps have been produced, due to the presence of significant ground spillover in the absolute maps. This is going to improve a lot with the analysis of the larger dataset already acquired and with future system developments.

The significant mismatch between the lowest multipoles sampled by interferometric measurements and the highest multipoles measured by BOOMERanG and MAXIMA is reduced to less than 2 σ once the beam error and the partial overlap of the ℓ-bands are taken into account. It is, however, a possible indication of a calibration systematic still

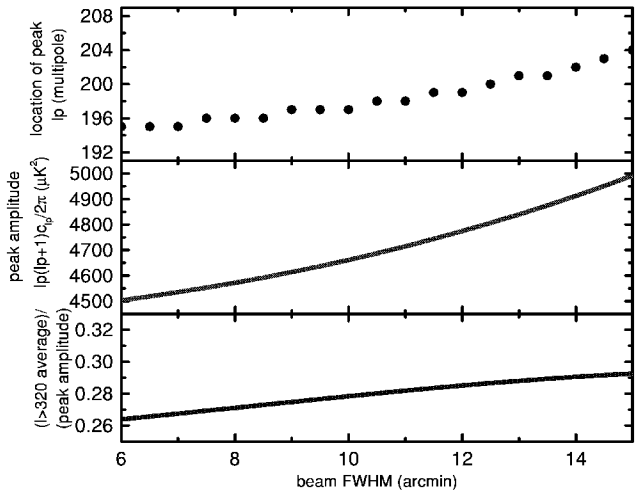

FIGURE 5. Effect of the beam FWHM on the most important characteristics of the power spectrum measured by BOOMERanG. The nominal FWHM is 10 arcmin.

unaccounted for.

The final measurements will arrive with the MAP (launch in a few months) and Planck (launch in 2007) satellite experiments. In the following we focus on what we can already say about the curvature.

COSMOLOGY FROM CMB ANISOTROPY

The position, amplitude and width of the peak evident in fig.4 are consistent with the general adiabatic inflationary scenario, while the simplest models based on topological defects do not fit the data as well.

Using a naive quadratic fit estimator for the MAXIMA and BOOMERanG data we find that the peak is located at multipole $\ell = (197 \pm 6)$ for BOOMERanG (1σ, bandcenters from 50 to 300, data from [32]) , $\ell = (233 \pm 33)$ for MAXIMA (1σ, bandcenters from 55 to 300, data from [33]) , $\ell = (195 \pm 8)$ for the combination of the two datasets (1σ, bandcenters from 65 to 296, data from [52]). These results can shift a little bit higher if one assumes skewed power spectra similar to the adiabatic scenario ones [53].

This location of the maximum is consistent with a flat geometry of space, but it is not univocally related to the density parameter Ω if we allow for a non vanishing cosmological constant [8]. Moreover, the location of the maximum alone is not the best way to constrain Ω, and there is much more information contained in the datasets. Jaffe et al.[52] carried out a full Bayesian analysis on the combined BOOMERanG, MAXIMA and COBE-DMR datasets, constraining simultaneously the parameters Ω, $\Omega_b h^2$, n_s, $\Omega_c h^2$.

It must be stressed that this kind of analysis assumes an adiabatic inflationary model. Moreover, it is very important to specify in detail the prior distributions assumed for each of the parameters. This is especially important in the case of CMB power spectrum measurements, since an important geometrical degeneracy is present [9], so different combinations of the parameters produce very similar power spectra. The 95% confidence intervals for Ω, taking into account all the degeneracies, range from $(0.88-1.12)$ to $(0.97-1.35)$ depending on the assumed priors and parametrizations [52, 10, 24]. This strongly suggests a flat geometry of the Universe, and at least implies, with 95% confidence, a curvature length

$$R = \frac{c}{H_o} \frac{1}{\sqrt{|\Omega - 1|}}$$

larger than 8.3 to 2.9 times the Hubble length.

Needless to say, having demonstrated that $\Omega \sim 1$ has very important cosmological consequences. According to several independent measurements and methods, the matter density parameter Ω_M is significantly smaller than unity and close to 30% [54, 55, 56, 57, 58]. This means that about 70% of the mass and energy present in the Universe must be in a different form: not ordinary matter, not dark matter.

The presence of dark energy (a form of repulsive energy with negative pressure) is an interesting hypothesis to solve the puzzle. Its presence has been independently proposed [7, 59, 60, 61, 62] to drive the acceleration of the expansion rate of the Universe hypotised to explain the observation of distant supernovae [63, 64]. This hypothesis is still widely debated, the main interpretation problem remaining the lack of a convincing particle physics model for the dark, negative pressure form of energy required.

In the same adiabatic perturbations framework, BOOMERanG and MAXIMA constrain the slope of the initial power spectrum of density perturbations n_s in the range 1.01 ± 0.17 (95% confidence) [52]. In addition to the Ω measurement, tese results for n_s are also consistent and support the simplest inflationary scenarios [65, 19, 66].

The third parameter constrained by BOOMERanG and MAXIMA is the density of baryons. In the power spectrum this parameter controls the relative amplitude of the first peak to the second one. From the power spectrum of fig.4, this ratio is constrained to be $\sim 2\sigma$ larger than expected for a standard primordial nucleosynthesis (BBN) ($\Omega_b h^2 = (0.019 \pm 0.002)$ from [67], $\Omega_b h^2 = (0.020 \pm 0.002)$ from [68]). This suggests a high physical density of baryons. Depending on the assumed priors, 95% intervals for $\Omega_b h^2$ ranging from $(0.019-0.045)$ to $(0.026-0.048)$ are obtained from the CMB power spectrum data. These results are only marginally overlapping the BBN one, but given the orthogonality of the methods and of the systematic errors, I would rather speak of good overall consistency of the model. It must be stressed, in fact, that the density of baryons enters in the two observable in completely different ways. It controls the primordial abundance of light elements due to its effect in the nuclear reactions happening in the first minutes after the big bang. It also affects the density oscillations (acoustic waves) producing CMB anisotropies about 300000 years after the big bang. Completely different physical phenomena at completely different regimes in the early history of the Universe require the density of baryons to be the same to within a factor 1.5: this should be considered a wonderfull success of cosmology. New physics will be required

only if future, more precise measurements will confirm and increase the present $\sim 2\sigma$ disagreement. Also, note that frequentist methods point to a statistical consistency of the two results [69].

BEYOND THE POWER SPECTRUM

At this point the next step is obvious: we should check if the detected temperature fluctuations are gaussian distributed, another prediction of inflation. This is very difficult to test, since instrumental effects can mask small cosmic non gaussianities, and can produce subtle non gaussianities as well. Moreover, different methods probe different kinds of non gaussianity (see e.g. [70] and references therein). A reality check, simply using the 1 point distribution of the BOOMERanG map, has been published in [40]: the detected pixel temperature fluctuations (normalized to the square root of the sum in quadrature of sky variance and instrument noise variance in that pixel) are indeed very precisely gaussian distributed. This is only a starting point in the demonstration of the gaussian character of the CMB, since the central limit theorem helps a lot in this kind of test. However, it is at least reassuring the fact that we do not detect deviations from gaussianity in the data at high latitudes at 150 GHz, while deviations are evident in the data at lower galactic latitudes at 150 GHz, and at all the latitudes in the dust dominated map at 410 GHz. A detailed non gaussianity analysis is underway. The MAXIMA team has already published a first analysis of gaussianity of the CMB map [71]. The main difficulty is, of course, to separate with high confidence small instrumental effects and foreground contaminations from real non-gaussian signatures in the CMB, if any. Realistic montecarlo simulations are the only way to assess the statistical significance of detections of (or upper limits to) non-gaussianity.

CMB Photons are last scattered by electrons at the recombination epoch. ItŠs a Thomson scattering. If the distribution of incoming radiation has a quadrupole moment, the scattered radiation has some degree of linear polarization. The degree of linear polarization is of the order of $\lesssim 10\%$ of the anisotropy: the expected signal is thus of the order of a few μK rms or less (see e.g. [72]). Despite a long lasting experimental effort (see e.g. [73, 74, 75, 76, 77, 78]) the polarization of the CMB has not been detected yet. The best upper limits to date are of the order of 6×10^{-6} in $\Delta T/T$ at angular scales around one degree. In the standard scenario [79] we expect acoustic peaks in the polarization power spectrum at $\ell \gtrsim 200$. The presence of tensor perturbations generated by inflation produces a curl component B in the CMB polarization field which adds to the curl-free E component described above. Measuring the power spectrum of polarization of the CMB is very important for several reasons. First, it provides four power spectra to measure: in addition to the $< TT >$ power spectrum of the anisotropy T, it is possible to measure the $< TE >$ anisotropy-polarization cross-spectrum; the pure polarization power spectrum $< EE >$ is more challenging, while the $< BB >$ component is even smaller and is non-zero only if gravity-waves were present at last scattering. Its detection would prove directly the physics of inflation. The $< EB >$ and $< TB >$ spectra are zero by parity. The BOOMERanG instrument has been modified including a new focal plane with polarization senitive bolometers: its new long duration flight (called B2K) is

scheduled for the end of 2001. The forecast sensitivity to polarization has been computed in [80]. Many other attempts to measure CMB polarization are in progress(see e.g. [81] and references therein), and a first detection is expected soon .

ACKNOWLEDGMENTS

The BOOMERANG project has been supported by the CIAR and NSERC in Canada, by Programma Nazionale Ricerche in Antartide, Universitá "La Sapienza", and Agenzia Spaziale Italiana in Italy, by PPARC in the UK, and by NASA, NSF OPP and NERSC in the U.S. We received superb field and flight support from NSBF and the USAP personnel in McMurdo.

REFERENCES

1. Peebles, P.J.E, and Yu J.T., 1970, Ap.J. 162, 815
2. Sunyaev, R.A. & Zeldovich, Ya.B., 1970, Astrophysics and Space Science 7, 3
3. Doroshkevich A.G., Zeldovich Ya.B., Sunyaev R.A., 1978, Soviet Astronomy, 22, 523
4. Silk J. & Wilson M. L. 1980, Physica Scripta, 21, 708
5. Hu W., Sugiyama N. & Silk J., 1997, Nature, 386, 37
6. Martínez-González E., Sanz J.L. & Silk J., 1990, ApJ, 355, L5
7. Weinberg S. , Rev. Mod. Phys. 61 1 1989
8. Weinberg S. astro-ph/0006276
9. G. Efstathiou and J. R. Bond, Mon. Not. R. Astron. Soc. **304**, 75 (1999).
10. Melchiorri A. and Griffiths L.M., astro-ph/0011147
11. Seljak, U. & Zaldarriaga, M. 1996, Ap.J. 469, 437
12. Lewis A., Stewart E., Lasenby A., astro-ph/9911176
13. Bucher, M., Moodley, K. & Turok, N. 2000, astro-ph/0007360
14. Smoot G.F. *et al.* , 1992, ApJ, 396, L1
15. Bennett C.L. *et al.* , 1996, ApJ, 464, L1
16. Guth A.H., 1982, Phil. Trans. R. Soc., A307, 141
17. Linde A., 1982, Phys.Lett., 108B, 389
18. Linde A., 1983, Phys.Lett., 129B, 177
19. Albrecth A. & Steinhardt P.J., 1982, Phys.Rev.Lett., 48, 1220
20. Guth A.H. 1997, The Inflationary Universe: The quest for a new theory of cosmic originis, Addison-Wesley, New York.
21. Kolb E.B. & Turner M., 1990,'The Early Universe', Addison-Wesley, New York
22. Kinney W., Melchiorri A., Riotto A., PRD in press, astro-ph/0007375 (2000)
23. Vilenkin A. & Shellard E.P.S., 1994, 'Cosmic Strings and other Topological Defects', Cambridge University Press
24. Bond. R., et al., The Quintessential CMB, Past and Future, Proc. of the CAPP2000 meeting, Verbier, astro-ph/0011379
25. J. R. Bond, G. Efstathiou and M. Tegmark, Mon. Not. R. Astron. Soc. **291**, L33 (1997) and references therein
26. Pospieszalski, M., IEEE-MTT-S Digest, 1369, (1992)
27. Pospieszalski, M., IEEE-MTT-S Digest, 1121, (1995)
28. Torbet E., et al., Ap.J., **521**, L79-L82 , (1999)
29. Miller A., et al., Ap.J., **524**, L1-L4 , (1999)
30. Mauskopf P., et al., Applied Optics, **36**, 765-771, (1997)
31. Mauskopf P., et al., Ap.J., **536**, L59-L62 (2000)
32. de Bernardis P., et al., Nature **404**, 955 (2000).

33. Hanany S., et al., Ap.J., **545**, L5-L9 (2000)
34. Delabrouille J. et al., MNRAS, **298**, 445-450 (2000)
35. de Bernardis P. & Masi S., 1998, in 'Fundamental parameters in cosmology', Proc. of the XXXIIIrd rencontres de Moriond (France), Trân Thanh Vân J., Giraoud-Héraud Y., Bouchet F., Damour T. & Mellier Y. eds., Editions Frontiéres, p.209
36. Piacentini F., et al., 2001, astro-ph/0105148
37. Crill B., et al., 2001, in preparation.
38. Borrill J. in 3K cosmology, Roma 1998, AIP CP 476, 277, (1999).
39. Prunet, S. et al., 2000, in "Energy densities in the Universe", Bartlett J., Dumarchez J. eds., Editions Frontieres, Paris - astro-ph/0006052
40. P. de Bernardis, et al., ŞFirst results from the BOOMERanG experiment Ť, Proc. of the CAPP2000 meeting, Verbier, July 2000, astro-ph/00011469
41. Masi S., et al. 2001, ApJ Letters in press, astro-ph/0101539
42. WOMBAT collaboration, 1998, see http://astron.berkeley.edu/wombat/foregrounds/radio.html.
43. Hivon E. et al., astro-ph/0105302
44. Padin et al., 2001, astro-ph/0012211
45. Dawson K.S. et al., 2000, astro-ph/0012151
46. http://astro.uchicago.edu/dasi/
47. http://astro.caltech.edu/ tjp/CBI/
48. http://www.mrao.cam.ac.uk/telescopes/vsa/index.html
49. http://www.archeops.org/
50. http://www.topweb.gsfc.nasa.gov/
51. P. de Bernardis, G. De Troia, L. Miglio "Calibration of balloon-borne CMB experiments" NEW ASTRONOMY REVIEWS, 43, 281-287, 1999.
52. Jaffe, A., et al., 2001, PRL, 86, 3475-3479
53. Knox L., Page L., Phys.Rev.Lett. 85 (2000) 1366-1369
54. Donahue M., Voit M, astro-ph/9907333
55. Bahcall N.A. et al, *Ap.J.* **541**, 1 (2000)
56. Blakesee J.P., et al., astro-ph/9910340
57. Juszkiewicz R., et al., *Science* **287**, 109 (2000)
58. Wittman et al., Nature, May 11 2000
59. Ostriker J.P., and Steinhardt P.J., *Nature*, **377**, 600 (1995)
60. Caldwell R.R., Dave R., Steinhardt P.J., *Phys. Rev. Lett.*, **80**, 1582 (1998)
61. Armendariz C., Mukhanov V., Steinhardt P.J., astro-ph/0004134 (2000)
62. Amendola L., astro-ph/0006300
63. Riess A.G. et al, *Ap.J.* **116**, 1009 (1998)
64. Perlmutter S. et al, *Ap.J.* **517**, 565 (1999)
65. Linde A.D., *Phys.Lett.* **108B**, 389, (1981)
66. Watson, G.S., astro-ph/0005003, (2000)
67. Tytler, D. et al. 2000, Physica Scripta submitted, astro-ph/0001318
68. Burles, S., Nollett, K.M. & Turner, M.S. 2000, astro-ph/0010171
69. Gawiser E., astro-ph/0105010 (in this book)
70. R. B. Barreiro, astro-ph/9907094
71. J.H.P.Wu et al., 2001, Tests for Gaussianity of the MAXIMA-1 CMB Map , astro-ph/0104248
72. Kaiser N., 1983, M.N.R.A.S., 101, 1169
73. Caderni N., et al., 1978, PRD, 17.
74. Lubin P., Smoot G., Ap.J., 245, 1
75. Lubin P., et al., Ap.J., 273, L51
76. Wollack et al., 1993, Ap.J., 419, L49
77. Netterfield B., et al., 1996, Ap.J., 445, L69.
78. Pisano G., New Astronomy Reviews, 2000, 43, 329-339
79. A. Melchiorri, N. Vittorio, astro-ph/9610029
80. Tegmark M. et al. Astrophys.J. 530 (2000) 133-165
81. Staggs, S. et al., astro-ph/9904062